molecular pharmaceutics

Article

pubs.acs.org/molecularpharmaceutics

Tracking Antibody Distribution with Near-Infrared Fluorescent Dyes: Impact of Dye Structure and Degree of Labeling on Plasma Clearance

Cornelius Cilliers,[†] Ian Nessler,[†] Nikolas Christodolu,[†] and Greg M. Thurber*[,‡]

[†]Department of Chemical Engineering and [‡]Department of Biomedical Engineering, University of Michigan, Ann Arbor, Michigan 48109, United States

Supporting Information

ABSTRACT: Monoclonal antibodies labeled with near-infrared (NIR) fluorophores have potential use in disease detection, intraoperative imaging, and pharmacokinetic characterization of therapeutic antibodies in both the preclinical and clinical setting. Recent work has shown conjugation of NIR fluorophores to antibodies can potentially alter antibody disposition at a sufficiently high degree of labeling (DoL); however, other reports show minimal impact after labeling with NIR fluorophores. In this work, we label two clinically approved antibodies, Herceptin (trastuzumab) and Avastin (bevacizumab), with NIR dyes IRDye 800CW (800CW) or Alexa Fluor 680 (AF680), at 1.2 and 0.3 dyes/antibody and examine the impact of fluorophore conjugation on antibody plasma clearance and tissue distribution. At 0.3 DoL, AF680 conjugates exhibited similar clearance to unlabeled antibody over 17 days while 800CW conjugates diverged after 4 days, suggesting AF680 is a more suitable choice for long-term pharmacokinetic studies. At the 1.2 DoL, 800CW conjugates cleared faster than unlabeled antibodies after several hours, in agreement with other published reports. The tissue biodistribution for bevacizumab−800CW and −AF680 conjugates agreed well with literature reported biodistributions using radiolabels. However, the greater tissue autofluorescence at 680 nm resulted in limited detection above background at low (~2 mg/kg) doses and 0.3 DoL for AF680, indicating that 800CW is more appropriate for short-term biodistribution measurements and intraoperative imaging. Overall, our work shows a DoL of 0.3 or less for non-site-specifically labeled antibodies (with a Poisson distribution) is ideal for limiting the impact of NIR fluorophores on antibody pharmacokinetics.

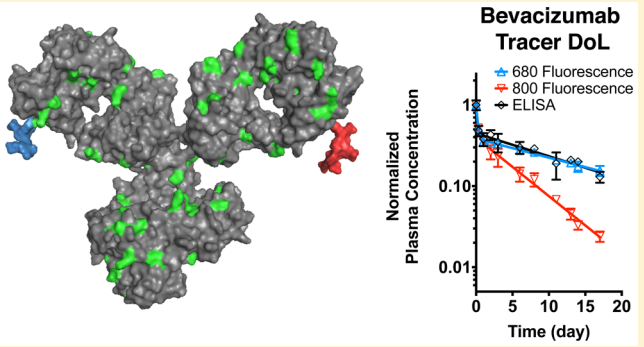

KEYWORDS: *IRDye800CW, Alexa Fluor 680, trastuzumab, bevacizumab, biodistribution, molecular imaging*

INTRODUCTION

Monoclonal antibodies are the largest class of biologics, and they continue to grow due to multiple applications in cancer treatment, autoimmune disorders, and other diseases. Currently there are over 50 FDA approved therapeutics, and as of mid-November 2015, there were 53 in phase 3 clinical trials and over 470 in various stages of the clinical pipeline.[1] Antibodies exhibit complex pharmacokinetics because of their large size, long circulating half-life (including FcRn recycling), target mediated drug disposition (TMDD), limited tumor penetration, and immunogenic responses, making *a priori* predictions of monoclonal antibody distribution exceedingly difficult. Therefore, robustly characterizing the pharmacokinetics of novel next-generation antibodies, antibody−drug conjugates, bispecific antibodies, and other protein scaffolds in the preclinical and clinical setting can aid in development and help produce lead therapeutic candidates with a higher likelihood of clinical success.

Bioanalytical methods remain the industry standard for measuring plasma clearance of biologics, since any modification (radiolabel, fluorophore, etc.) can potentially modify the distribution of an agent.[2,3] Conventional techniques for determining antibody disposition include plasma clearance measurements using ELISA or LC-MS, and tissue distribution using immunohistochemistry and immunofluorescence. However, these bioanalytical techniques do not have the high spatial and temporal resolution, the ease of measuring drug metabolism, or the direct detection of radiolabeling or fluorescence techniques. Radiolabeling methods made significant improvements during early studies with monoclonal antibodies (e.g., ref 4) in the stability of the conjugation chemistry and without disrupting binding.[5] Several results have shown negligible changes in plasma clearance relative to unlabeled antibodies.[6,7] Therefore, radiolabels remain the gold standard for quantifying bulk organ and tissue distributions using scintillation counting and *in vivo* imaging, such as positron emission tomography (PET).[8] Although experimental

Received: December 2, 2016
Revised: March 1, 2017
Accepted: March 15, 2017
Published: March 15, 2017

DOI: 10.1021/acs.molpharmaceut.6b01091
Mol. Pharmaceutics 2017, 14, 1623−1633

methods are approaching the cellular scale,[9] their resolution is intrinsically limited by the path length of the positron and imaging equipment. Additionally, the time/half-life constraints, safety concerns, and expense of radioactivity limit its broad applicability for high-resolution imaging and single-cell measurements.

There is growing interest in using near-infrared (NIR) fluorescent dyes as molecular imaging agents for pharmacokinetic tracking, disease characterization/detection,[10] and intraoperative imaging[11,12] due to the high spatial and temporal resolution of fluorescence imaging, low tissue autofluorescence, and deep tissue penetration of NIR light.[13−17] For example, in a recent publication, we used the high spatial resolution of fluorescence to demonstrate the importance of tumor penetration on antibody drug conjugate (ADC) efficacy, highlighting one application where tissue-level distribution in addition to organ-level biodistribution is important for describing drug effects.[18] NIR dyes provide a convenient and safe method to quantify pharmacokinetics at the subcellular to tissue level while retaining the possibility for quantifying macroscopic organ biodistribution (e.g.,[19] although more tissue processing is required compared to radiolabeling). Radiolabeling techniques remain the gold standard for whole animal imaging and organ biodistribution due to the higher scattering and absorption of fluorescent light. However, NIR fluorescent dyes can complement these results with high-resolution tissue distribution (fluorescence microscopy) and single-cell data (flow cytometry) while providing biodistribution data for validation between the methods (i.e., comparing fluorescence % ID/g[20] with radiolabeled results). Additionally, conventional visible light dyes can easily be used with NIR dyes for multichannel flow cytometry or immunofluorescence.[21]

Despite these advantages for high-resolution and single-cell imaging, NIR fluorescence labeling techniques have room for improvement to lower the impact of labeling on distribution and clearance (just as radiolabeling techniques did decades ago[6,22−24]). In particular, there is no consensus on the optimum degree of labeling (DoL), also known as the dye to protein ratio (D/P) or average number of dyes per antibody, that should be used to prevent the dye from altering antibody pharmacokinetics. Some recent work with the NIR fluorophore IRDye800CW (800CW, LI-COR) demonstrates that antibody clearance can be altered upon fluorophore conjugation,[6,20,25,26] and higher degrees of labeling result in increased liver uptake. While the benefit of higher signal often outweighs the cost of faster clearance for imaging and detection applications, it would limit the use for pharmacokinetic characterization of antibodies. These groups also showed that lower degrees of labeling result in a reduced impact on distribution; however, some of these studies were performed with dual radiolabeled and fluorophore labeled antibodies, thereby preventing independent comparisons between unlabeled and labeled antibodies.

In this work, we examined the effects of conjugation of 800CW and another commonly used fluorophore, Alexa Fluor 680 (AF680), on the pharmacokinetics of two clinically approved antibodies, Herceptin (trastuzumab) and Avastin (bevacizumab). We selected 800CW because of its clinical relevance for NIR intraoperative imaging and literature precedent and compared it to AF680 (excited in far-red and emitting in near-infrared) because of the similar cyanine based structures and residualization properties.[27] Our previous work with NIR labeled peptidomimetics also showed that AF680 has one of the lowest plasma protein binding rates of all the NIR dyes tested.[28] We used a 1.2 and 0.3 DoL of each dye, measured plasma clearance by fluorescence and ELISA, and performed tissue biodistribution experiments to see if fluorophore conjugation altered antibody distribution. Additionally, we labeled the clinically approved antibody−drug conjugate (ADC) Kadcyla (ado-trastuzumab emtansine) with AF680 and tracked its tumor distribution out to 7 days as an example application studying tissue pharmacokinetics.

MATERIALS AND METHODS

Antibodies and Imaging Agents. Trastuzumab (Herceptin, Roche), bevacizumab (Avastin, Roche), and ado-trastuzumab emtansine (T-DM1, Kadcyla, Roche) were obtained from the University of Michigan pharmacy. Alexa Fluor 680 NHS Ester (AF680, ThermoFisher Scientific) and IRDye800CW (800CW, LI-COR) were conjugated to each antibody following the manufacturers' instructions as previously described.[18,27] Briefly, dyes were reacted at an antibody concentration of 2 mg/mL in PBS with 10% sodium bicarbonate (v/v) for 2 h at 25 °C and then purified using Biogel *P*-6, Fine (Bio-Rad) in Spin-X centrifuge filter tubes (Corning).[27] Dye to antibody molar ratios of 3.0 and 0.5 were used to obtain the 1.2 and 0.3 degrees of labeling, respectively. The degree of labeling was determined by using a NanoDrop 2000c spectrophotometer (ThermoFisher Scientific) to measure fluorophore absorption and the protein absorbance at 280 nm, corrected for the fluorophore. The degree of labeling is defined as the average dye to protein concentration ratio. Sample absorption spectra are included in the Supporting Information (Figure S1). After purification, conjugates were run on SDS-PAGE and scanned on an Odyssey CLx to ensure all free dye was removed (Figure S2). Binding affinities were performed as previously described[3] using HCC1954 cells. Briefly, titrations of unlabeled antibody and antibody−dye conjugates were incubated with 50,000 HCC1954 cells on ice for 3 h and washed. After the primary incubation, cells were further incubated with antihuman IgG Fc-AlexaFluor488 at 40 nM for 30 min on ice, washed, and subsequently run on an Attune Focusing Cytometer (Applied Biosystems). K_d was estimated using PRISM and is reported as $K_d \pm$ standard error.

Plasma Clearance. All animal studies were approved and conducted in compliance with the Institutional Animal Care and Use Committee (IACUC) of the University of Michigan. Animal studies were conducted in C57BL/6J or Foxn1 nude (Jackson Laboratories) mice. Plasma clearance was measured after tail-vein injection of 500 μg of unlabeled stock antibody with 50 μg of labeled antibody at the different DoL's described above (N = 3 for each DoL). Plasma concentration was determined by fluorescence and ELISA for each sample. Plasma samples were obtained through retroorbital sampling 10 μL of whole blood, mixing with 15 μL of PBS-EDTA (10 mM), centrifugation at 3000*g* for 1 min, and freezing 18 μL of the resulting plasma. The concentration of fluorescent antibody was determined by scanning 15 μL of plasma on the NIR Odyssey CLx Scanner (LI-COR) and comparing the signal intensity to a calibration curve of known concentration to signal intensity at the same scan settings. Plasma concentration as measured by fluorescence and ELISA was normalized to the initial value, and then the clearance was fit to a biexponential decay using PRISM (GraphPad). Absolute plasma concentrations at 1 min were compared with theoretical initial concentrations based on the dose and estimated plasma volume of the mouse. The area under the curve (AUC) for normalized

DOI: 10.1021/acs.molpharmaceut.6b01091
Mol. Pharmaceutics 2017, 14, 1623−1633

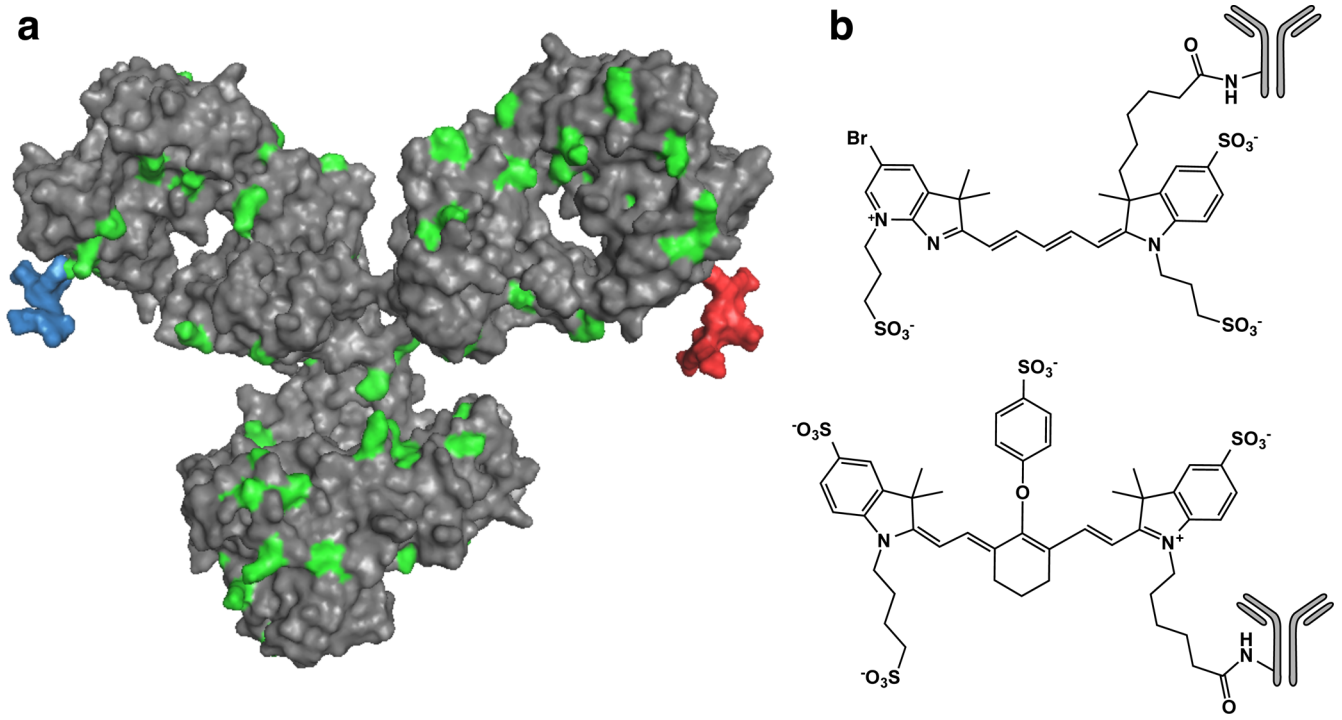

Figure 1. Space filling model of an IgG (PDB ID: 1igy)[32] with both AF680 (blue) and 800CW (red) attached to lysines (green) on the heavy chain (A). Dye structures were exported from MarvinSketch as a pdb file and merged with the IgG in Pymol. (B) Chemical structure of AF680 (top) and 800CW (bottom).

clearance for ELISA and fluorescence was determined for each conjugate at 3 and 17 days using the trapezoidal rule. The normalized fluorescence AUC was compared to normalized ELISA AUC by a one tailed, paired Student's t test, and a significance level of $p < 0.05$ was considered significant.

Total Antibody ELISA. Immulon IV 96 well plates (Fisher Scientific, 14-245-153) were coated with mouse antihuman IgG Fc antibody (BioLegend, 409302) overnight at 4 °C and 1 μg/mL in PBS. Wells were then washed 3 times (PBS with 0.05% Tween-20), blocked with 2% PBS-BSA, 0.05% Tween-20 for 2 h at room temperature, and washed 3 more times. Samples were diluted at least 1:100 in diluent (PBS, 1% BSA, 0.05% Tween-20) and incubated for 1 h at room temperature. After sample incubation, plates were washed 3 times, and the detection antibody, mouse antihuman IgG Fc HRP (Southern Biotech, 9040-05), was diluted 1:10000 in diluent, added to each well, and incubated for 1 h at room temperature. Plates were then washed 4 times and developed using TMB substrate (Fisher Scientific, ENN301). Assay ranges for both trastuzumab and bevacizumab were between 6 ng/mL and 1.2 μg/mL.

Biodistribution. The biodistribution of bevacizumab conjugates was determined as previously described.[18,19,29] Briefly, 48 h after tail-vein injection of 50 μg of bevacizumab−dye conjugate (assumed to be in a linear clearance range due to no target binding and negligible Fc receptor saturation), animals were euthanized and organs were resected. Organs were then homogenized by mechanical disruption, incubated with RIPA buffer (Fisher Scientific, NC9517624)/PBS solution supplemented with 6 mg/mL collagenase IV (Fisher Scientific, NC9919937) for 1.5 h, disrupted using a FB-120 Sonic Dismembrator, and incubated in RIPA buffer/0.025% trypsin-EDTA solution for 1.5 h. After homogenization, organs were serially diluted and scanned on the Odyssey CLx scanner to ensure fluorescence detection was in the linear range. The signal intensity was compared to a calibration curve and normalized to organ weight and homogenate volume in order to compute the percent injected-dose per gram (%ID/g). Calibration standards were made in mouse plasma and subjected to the same incubations above. The signal-to-noise ratio (SNR) was also calculated for each organ. The SNR is defined as the organ fluorescence minus the autofluorescence signal from control (uninjected) mice divided by the standard deviation of autofluorescence from the control mice. The %ID/g for each organ for Bev-AF680 and Bev-800CW was compared by a two-tailed, paired Student's t test. Each organ for Bev-AF680 and Bev-800CW was compared to Paudyal et al.[30] by a two-tailed, unpaired Student's t- test. A significance level of $p < 0.05$ was considered significant.

Fluorescence Histology of Antibody Distribution. As previously described,[18,21] the tumor distribution of T-DM1-AF680 was analyzed using fluorescence microscopy at 1, 3, 5, and 7 days. Briefly, nude mice were inoculated with 5×10^6 NCI-N87 cells in the rear flanks and the clinical dose (3.6 mg/kg) of T-DM1-AF680 was administered via tail-vein injection once the longest axis of the tumor was approximately 10−12 mm. Before euthanizing mice at the aforementioned times, Hoechst 33342 (ThermoFisher Scientific, H3570) was administered via the tail-vein at 15 mg/kg to label functional vasculature in the tumor.[31] After euthanizing the mice, tumors were resected, flash frozen in OCT using isopentane chilled on dry ice, and cut for histology on a cryostat (16-μm slices). Before imaging, slices were stained with antimouse CD31 (BioLegend, 102402) conjugated with Alexa Fluor 555, and mouse antihuman IgG Fc antibody (BioLegend, 409302) conjugated with Alexa Fluor 488. Microscopy was performed using an upright Olympus FV1200 confocal microscope equipped with a 20× objective and 405, 488, 543, and 635

DOI: 10.1021/acs.molpharmaceut.6b01091
Mol. Pharmaceutics 2017, 14, 1623−1633

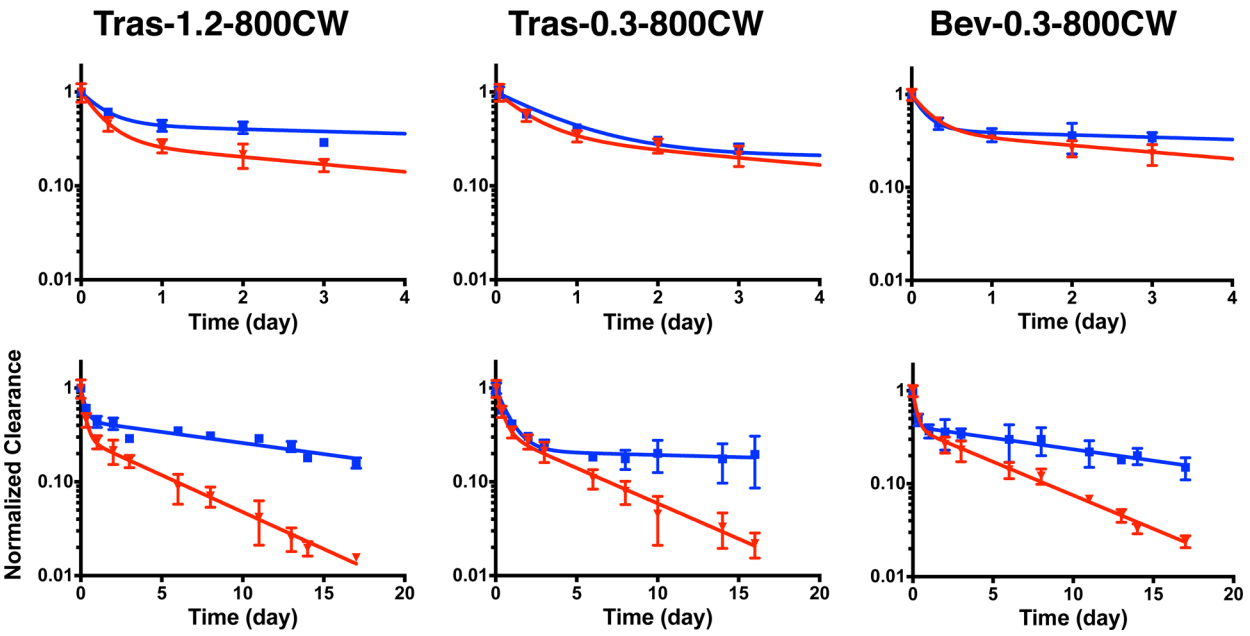

Figure 2. Antibody−800CW conjugate plasma clearance. Normalized clearance as measured by fluorescence (red) and ELISA (blue) for trastuzumab with a DOL of 1.2 and 0.3 (left and middle, respectively), and bevacizumab with a 0.3 DOL (right) for 800CW conjugates. Clearance over the first 4 days is shown on top. Trast, trastuzumab; Bev, bevacizumab.

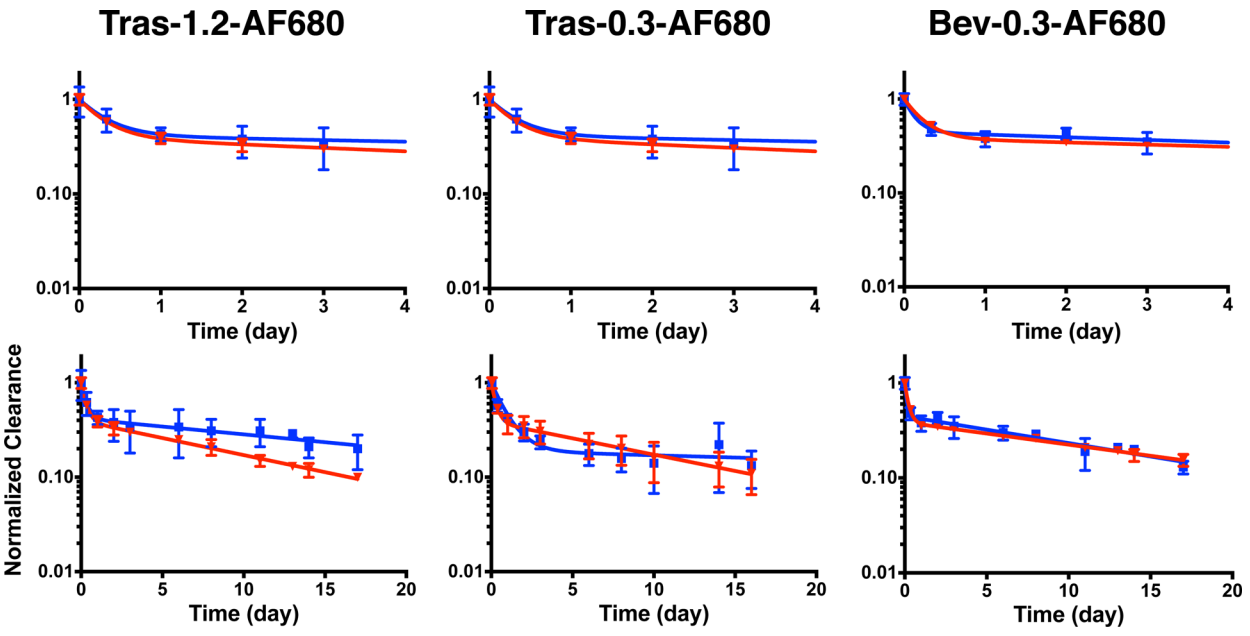

Figure 3. Antibody−AF680 conjugate plasma clearance. Normalized clearance as measured by fluorescence (red) and ELISA (blue) for trastuzumab with a DoL of 1.2 and 0.3 (left and middle, respectively), and bevacizumab with a 0.3 DoL (right) for AF680 conjugates. Clearance over the first 4 days is shown on top. Trast, trastuzumab; Bev, bevacizumab.

lasers (Figure S5). Tumor images were obtained by stitching smaller images with the Olympus software. Images were exported and analyzed using ImageJ image analysis software as described previously.[18,21]

RESULTS

A space-filling model of a full IgG1 antibody (PDB code: 1igy)[7,32] (gray) conjugated to a single molecule of AF680 (blue) and 800CW (red) shows the relative size difference between a typical antibody and dye (Figure 1a). Both dyes are shown nonspecifically conjugated to lysines on the heavy chain of the antibody. Lysines, which are a common site for nonspecific conjugation of small molecules or fluorescent dyes using ester chemistry, are shown in green. (The number and placement of lysine residues will vary between antibodies.) For bevacizumab and trastuzumab there are 86 and 90 lysines, respectively, with a majority appearing on the heavy chain (62 and 64, respectively).[33] Figure 1b shows the chemical structure of AF680 and 800CW conjugated to the amine of a lysine on the antibody.[34] Both cyanine dyes share a similar structure and have similar hydrophilicity; however, AF680 has one less sulfate group, giving it a net −2 charge compared to 800CW's net −3

DOI: 10.1021/acs.molpharmaceut.6b01091
Mol. Pharmaceutics 2017, 14, 1623−1633

charge. Also, the optical properties for AF680 and 800CW make them ideal for use with the 700 and 800 channels of the Odyssey CLx, respectively.

After conjugation and purification, all antibody−dye conjugates were run on SDS-PAGE and the gel was scanned on the Odyssey CLx to ensure free dye was removed (Figure S2). This indicates less than 3% free dye remaining.[35] Differences in relative labeling of the heavy or light chain could cause differences in antibody pharmacokinetics between the dyes; however, the relative intensities of heavy to light chain are similar, indicating any observed differences are likely due to the dye and not differences in labeling location. Absorbance spectra used for DoL characterization are included in the Supporting Information (Figure S1).

Plasma clearance for each antibody−dye conjugate was determined by fluorescence and the total antibody clearance by ELISA. The plasma concentration as measured by fluorescence and ELISA was normalized to the initial concentration and fit to a biexponential decay using PRISM. Table S1 in the Supporting Information shows the fitted parameter values. Figures 2 and 3 show the normalized plasma clearance and biexponential fits over 4 days (top) and 17 days (bottom). The absolute plasma concentration time profiles are shown in Figure S6. At a 1.2 DoL, the fluorescent Tras-800CW exhibited faster clearance than the total trastuzumab, even 8 h postinjection (which have nonoverlapping error bars) (Figure 2). At longer times, the beta phase clearance diverges significantly, indicating 800CW altered the pharmacokinetics of the antibody. These data agree with Conner et al.,[6] where the clearance of a different antibody−800CW conjugate showed faster clearance at a similar DoL of 1.5. At a 0.3 DoL, however, both Tras-800CW and Bev-800CW showed similar clearance over the first several days, and only after 4 days does the clearance diverge significantly. The AUC for the normalized plasma clearance (Table 1) shows the fluorescence AUC is significantly different from the total antibody AUC for all 800CW conjugates at 17 days. The serum stability of Tras-AF680 and Tras-800CW was also measured over 17 days (Figures S3 and S4). Tras-AF680 and Tras-800CW maintain 95% and 85% of their initial signal at day 4 and >80% and >60% by day 17, respectively, indicating serum stability/dye quenching is not the cause of faster clearance. The lack of free dye formation in plasma (Figure S7) and serum stability samples indicates that dye deconjugation is likely not causing the faster clearance of fluorescent antibody.

Table 1. Normalized AUC for Antibody-Dye Conjugates

Conjugate	$AUC_{day\ 0-3}$ (day)	$AUC_{day\ 0-17}$ (day)
Tras-1.2-800-F	**0.92 ± 0.03**[a]	**1.77 ± 0.07**[a]
Tras-1.2-800-E	**1.41 ± 0.39**	**4.92 ± 1.16**
Tras-1.2-680-F	1.26 ± 0.15	3.81 ± 0.41
Tras-1.2-680-E	1.39 ± 0.38	5.45 ± 1.82
Tras-0.3-680-F	1.27 ± 0.25	3.69 ± 1.10
Tras-0.3-680-E	1.26 ± 0.06	3.59 ± 0.92
Tras-0.3-800-F	1.13 ± 0.18	**2.14 ± 0.48**[a]
Tras-0.3-800-E	1.26 ± 0.03	**3.77 ± 0.53**
Bev-0.3-680-F	1.24 ± 0.06	4.48 ± 0.25
Bev-0.3-680-E	1.33 ± 0.15	4.70 ± 0.59
Bev-0.3-800-F	1.11 ± 0.06	**2.45 ± 0.16**[a]
Bev-0.3-800-E	1.24 ± 0.20	**4.70 ± 1.08**

[a]Fluorescence and ELISA AUC are significantly different ($p < 0.05$).

In comparison, AF680 exhibits less impact on the pharmacokinetics of the antibodies (Figure 3). Even at a 1.2 DoL, Tras-AF680 shows similar clearance to total antibody out to 9 days. At a 0.3 DoL, both trastuzumab and bevacizumab exhibited similar clearance over 17 days. Although the biexponential fit for Tras-AF680 appears to have a faster beta phase decay, the data points are overlapping at each point. For Bev-AF680, the clearance is nearly identical. Furthermore, the fluorescence AUC does not differ significantly from total antibody for any AF680 conjugates (Table 1), even at the higher DoL. These results indicate a 0.3 DoL of AF680 does not significantly affect antibody disposition for these antibody−dye conjugates.

For non-site-specific labeling techniques, such as conjugation to surface lysine residues using *N*-hydroxysuccinimide (NHS) chemistry, the number of possible labeling sites is relatively large. Therefore, the number of dyes per antibody is anticipated to result in a Poisson distribution.[36−38] Assuming the nonspecific lysine conjugation of fluorophores follows this distribution, Figure 4a shows the expected fractions of the number of dyes per antibody in samples with a DoL of 0.3 and 1.2. For the 0.3 DoL, the distribution of antibody labeling is approximately 75% unlabeled, 22% singly labeled, and <5% with 2 or more dyes per antibody. At the higher DoL of 1.2, the fraction of unlabeled antibody decreases (30%) and the percentage of singly labeled increases (36%); however, the fraction of antibody with 2 or more labels also dramatically increases to 44%. When using fluorescence detection, the unlabeled antibodies do not contribute to the overall signal, and antibodies with 2 dyes would contribute twice as much signal (assuming no quenching effects). Accounting for these two phenomena, Figure 4b and 4c show the expected theoretical contributions to the overall fluorescent signal from a DoL of 0.3 and 1.2 (assuming no self-quenching). For a DoL of 0.3, 74% of the measured fluorescence signal is expected to be from antibodies with a single dye, while only 30% of the signal is expected to be from singly labeled antibodies at a DoL of 1.2. Importantly, the percentage of signal from antibodies with 3 or more dyes is less than 4% of the total signal for a DoL of 0.3. Conversely, over a third of the signal for DoL 1.2 comes from 3 or more dyes per antibody. The 1.2 DoL also caused a slight increase in the K_d compared to no difference with 0.3 DoL (Figure 4d,e).

Reduced autofluorescence in the NIR region of the electromagnetic spectrum has prompted the use of NIR fluorescent dyes in tissue biodistribution studies with the Odyssey CLx scanner.[6,18,19,29] Whole organ fluorescence scans suffer from depth of imaging artifacts and provide arbitrary values (requiring the digest and dilution for absolute quantification) but agree qualitatively with the organ digest results (Figure S8). Previous studies have compared 800CW to radiolabels and have found antibody disposition is not significantly altered at sufficiently low DoL.[20,25] Because tissue autofluorescence is higher in the 680 nm region of the spectrum (relevant for AF680) compared to the 800 nm region, we chose to compare the biodistribution of AF680 and IRDye labeled antibodies. To limit variability between animals, we compared the distribution in the same mice using both the 700 and 800 channels on the Odyssey CLx (since there is negligible cross talk between the dyes in the different channels). The biodistribution of Bev-AF680 and Bev-800CW, both with a 0.3 DoL, 48 h after IV administration is shown in Figure 5a. For comparison, the biodistribution 48 h after tail-vein injection of

DOI: 10.1021/acs.molpharmaceut.6b01091
Mol. Pharmaceutics 2017, 14, 1623−1633

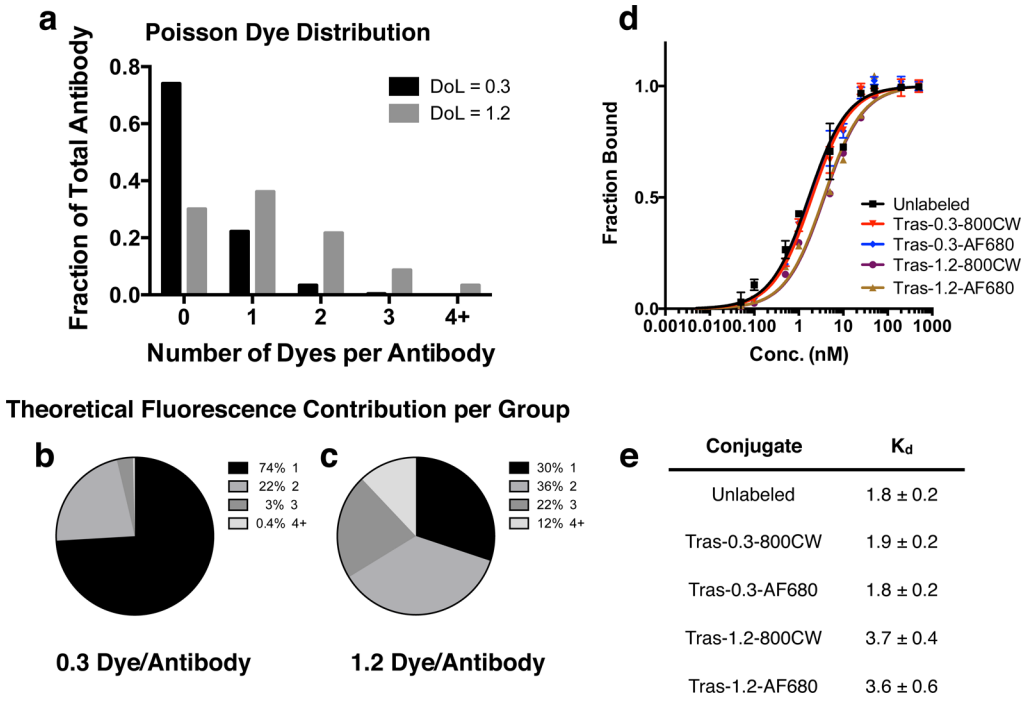

e

Conjugate	K_d
Unlabeled	1.8 ± 0.2
Tras-0.3-800CW	1.9 ± 0.2
Tras-0.3-AF680	1.8 ± 0.2
Tras-1.2-800CW	3.7 ± 0.4
Tras-1.2-AF680	3.6 ± 0.6

Figure 4. Theoretical dye per antibody distribution and fluorescence contribution. (A) Expected number of dyes per antibody for DoL 1.2 and 0.3, assuming Poisson distribution. Theoretical fluorescence contribution for antibodies with 1, 2, 3, or 4+ dyes per antibody at a 0.3 (B) and 1.2 (C) DoL. (D, E) Binding curves and affinities of unlabeled trastuzumab− and trastuzumab−dye conjugates. Tras, trastuzumab.

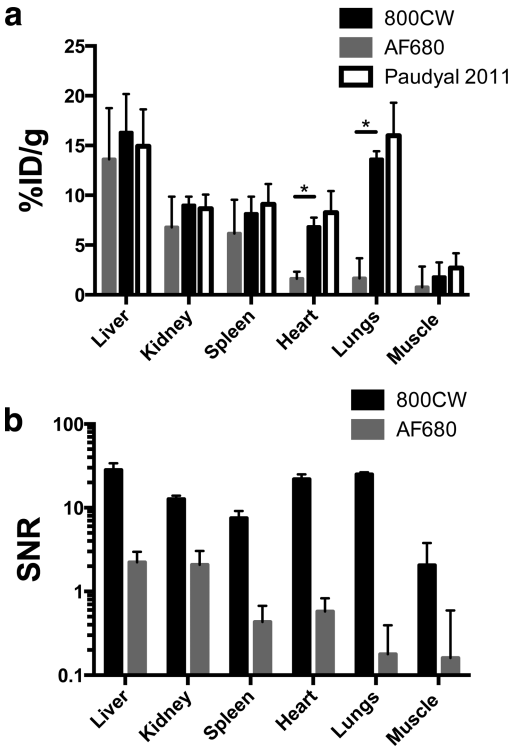

Figure 5. Bevacizumab biodistribution at 0.3 DoL. (A) Biodistribution of Bev-800CW and Bev-AF680 48 h post tail-vein injection. Signal to noise ratio (SNR) in each organ for 800CW and AF680.

radiolabeled bevacizumab was plotted from Paudyal et al.[30] This data set was chosen because of the matching times, use of a residualizing label (as are IRDye800CW and AF680[27]), and lack of flushing the organs (which will remove blood signal but could also alter tissue values). Paudyal and colleagues quantified the distribution of a 20 μg dose of ^{64}Cu-DOTA-bevacizumab after blocking any specific interactions.[30] The biodistribution of Bev-800CW agrees well with the radiolabeled data, with no significant differences between any of the organs. Although 800CW appears to impact antibody clearance over longer times, at 48 h the similar plasma clearance (Figures 2 and 3) and systemic distribution (Figure 5) do not appear to significantly alter the distribution at a 0.3 DoL. The Bev-AF680 distribution also agrees well with the radiolabeled data for the liver, kidney, and spleen; however, the signal-to-noise ratio (SNR) is less than or equal to one (Figure 5b) for several organs because of the higher autofluorescence in the 700 channel, the 0.3 DoL, and the moderate dose (~2.0 mg/kg). In particular, the heart and lungs show much lower uptake for Bev-AF680 likely, because the detectable signal is still in the range of background autofluorescence for this dosing level, resulting in a significant difference from Bev-800CW and ^{64}Cu-DOTA-bevacizumab.[30] For the liver and kidney, the SNR is higher and a specific signal can be detected over the background. The lower autofluorescence and correspondingly high SNR for all of the organs make 800CW more suitable for whole organ distribution studies. AF680 at a 0.3 DoL may also be used in organ biodistribution studies, but to improve the SNR ratio in some organs may require higher doses than the 50 μg/mouse dose used in this study.

Despite the higher autofluorescence in whole organ biodistribution experiments, the AF680 signal is high enough to detect the distribution of antibodies in tumors by histology following clinical doses (e.g., 3.6 mg/kg for ado-trastuzumab emtansine/Kadcyla). As an application of the direct detection provided by NIR fluorophores, we conjugated AF680 to the clinically approved antibody−drug conjugate (ADC) T-DM1 and tracked the tumor distribution over 1 week. Administration of T-DM1-AF680 at the clinical dose of 3.6 mg/kg resulted in a heterogeneous distribution in NCI-N87 tumor xenografts

DOI: 10.1021/acs.molpharmaceut.6b01091
Mol. Pharmaceutics 2017, 14, 1623−1633

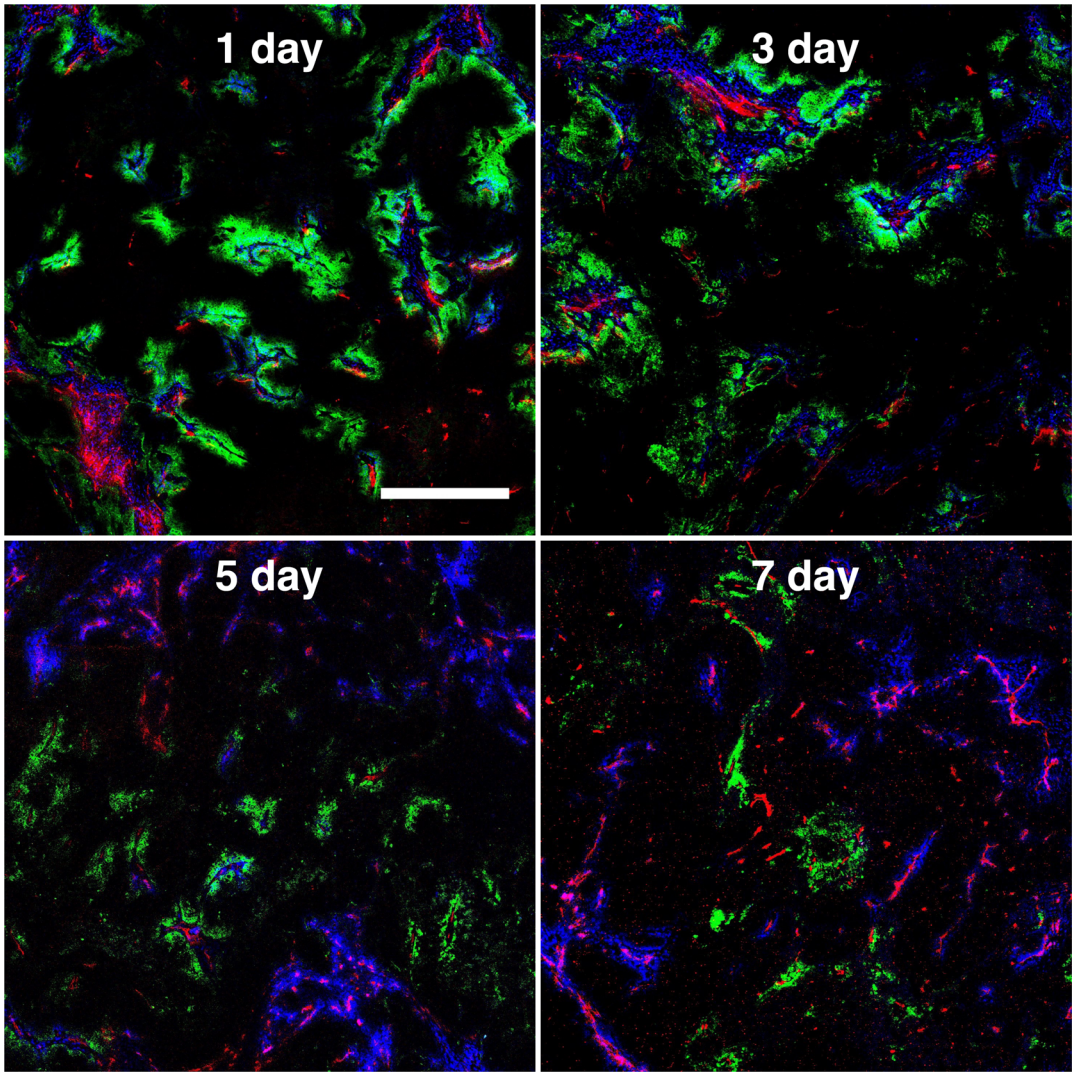

Figure 6. Fluorescent tumor histology following injection of a clinical dose (3.6 mg/kg) of T-DM1-AF680 (green) imaged at 1, 3, 5, and 7 days postinjection. Thirty min prior to sacrifice, Hoechst 33342 (blue) was injected at 15 mg/kg to highlight functional vasculature. *Ex vivo* staining was done with antimouse CD31-AF555 (red) to show all (functional and nonfunctional) tumor vasculature. Scale bar is 500 μm. Window leveling is different for each image.

(Figure 6). Injection of Hoechst 33342 and immunofluorescence staining with antimouse CD31 further show that the antibody disposition is limited to cells adjacent to tumor vasculature. The heterogeneous and perivascular distribution of the intact and internalized antibody (AF680 is a residualizing dye[27]) is maintained over 7 days, while anti-Fc staining shows a loss of intact antibody (Figure S5). This is consistent with the continuous internalization and degradation of HER2,[39] which results in antibody targeting cells close to the vessels and a majority of the tumor never receiving the therapeutic.[40]

DISCUSSION

Here we present a study of two commonly used NIR fluorophores (Figure 1) and their effects on the pharmacokinetics of two clinically approved antibodies. The goal of the investigation was to identify labeling conditions with a minimal impact on antibody distribution for use in pharmacokinetic studies. Our results agree with other literature reports of 800CW causing increased antibody clearance and altered tissue distribution (compared to unlabeled or radiolabeled antibodies) at DoLs greater than 1.0 (Figure 2) but lower impact at early times (<4 days) at tracer levels (DoL = 0.3 or less). Building on these results, we tested an additional NIR fluorophore, AF680, which has reduced plasma protein binding compared to 800CW.[28] AF680 antibody−dye conjugates showed nearly identical plasma clearance compared to unlabeled antibodies at 0.3 DoL, and even at 1.2 DoL did not have a significantly different normalized AUC (Figure 3, Table 1). These results should help clarify conflicting reports in the literature, delineate the impact of NIR labeling on plasma clearance, biodistribution, and tissue penetration studies, and aid in the selection of labeling conditions for different applications. In particular, the ability of fluorescence to provide cellular and subcellular resolution images (e.g., histology) and quantitative single-cell data (e.g., flow cytometry) makes fluorescence an attractive technique for providing high-resolution pharmacokinetic data that cannot be obtained by other current methods.

Both dyes have relative strengths and weaknesses highlighted by these results. IRDye800CW is currently being tested in the clinic with antibodies (e.g., Trial: NCT01508572), making it an attractive option for antibody labeling. (The only FDA approved cyanine dye, indocyanine green (ICG), does not

DOI: 10.1021/acs.molpharmaceut.6b01091
Mol. Pharmaceutics 2017, 14, 1623−1633

have a functional group for labeling. After NHS ester functionalization, fluorescence is significantly quenched after antibody conjugation.[41]) The maximum uptake of antibodies in tumors often occurs after only a couple days, so for imaging and diagnostic applications the negligible impact of 800CW at short times (less than 4 days) would have a low impact during this time. In fact, a higher DoL will likely maximize tumor signal, which is important for depth of detection.[42,43] The increase in signal from the larger number of dyes per antibody outweighs the reduction in signal from lower tumor uptake (%ID/g) due to faster clearance. However, 800CW's impact on antibody disposition at longer times may limit its broad applicability in studying the pharmacokinetic distribution of antibodies. Conversely, AF680 may be a more suitable choice for antibody clearance studies (provided the DoL is low) and tissue distribution studies at longer time periods (e.g., greater than 4 days) despite having greater autofluorescence than 800CW. The higher 680 nm tissue autofluorescence, however, makes AF680 less appropriate for biodistribution studies at low doses and low degrees of labeling.

When labeling an antibody with any fluorophore for *in vivo* delivery, these results highlight the importance of keeping the DoL low to maximize the signal from singly labeled proteins (Figure 4). The ease of labeling proteins non-site-specifically with NHS-ester/lysine chemistry make this convenient for studying antibody distribution in preclinical models. The large number of surface accessible lysines, however, results in a Poisson distribution. Because any unlabeled antibodies are not fluorescently detected and antibodies labeled with 2 or more dyes have approximately twice (or more) the fluorescence as a singly labeled antibody, the total signal is skewed toward antibodies with several dyes, which are more likely to have altered distribution. Figure 4 shows that although the 1.2 DoL has an average of ∼1 dye per antibody, the Poisson distribution results in a surprising 70% of the fluorescence signal coming from antibodies with 2 or more dyes. While the Poisson distribution is well-known, once the unlabeled antibodies and weighting of the fluorescence signal is taken into account, it is somewhat striking that an average DoL of 1 is too high for measuring singly labeled antibodies. Overlabeling antibodies with radiolabels, small molecules, or fluorescent dyes has been shown to cause rapid clearance;[5,7,23,44,45] therefore, maximizing the signal from singly labeled antibodies by using a DoL of 0.3 or less is critical for applications requiring negligible impact on clearance. For both 800CW and AF680, these results indicate a DoL of 0.3 or less has the least impact due to less than 5% of the total signal coming from antibodies with 3 or more dyes. Although using a lower DoL results in less overall signal, the negligible background in the NIR, and the exceptional brightness and photostability of these dyes make both practical options for protein distribution studies. Alternatively, site-specific labeling, such as maleimide-cysteine chemistry, may give improved pharmacological behavior[46,47] and signal, but these techniques typically require modification of the antibody amino acid sequence, which could also alter stability, distribution, and clearance.

Several other groups have examined 800CW as a tool for tracking antibody disposition. Cohen et al. studied the effects of fluorophore labeling on an ^{89}Zr labeled antibody and showed antibodies with 0.5 dyes per antibody did not show significantly different biodistribution than cetuximab or bevacizumab with only the radiolabel.[20,25] As they increased the DoL for 800CW, the biodistribution started to diverge from the lower DoL and radiolabeled-only antibodies. In particular, liver uptake increased and other organ uptake decreased with higher 800CW DoL for both bevacizumab and cetuximab.[20,25] These results suggest a sufficiently high DoL of 800CW causes increased liver uptake, consistent with other reports showing increased hepatic uptake of radiolabels with high DoL's.[22] However, as Conner et al. mentioned, even at lower DoL, the effects of 800CW may be masked by the radiolabel/desferal moiety.[6] These authors studied differences in plasma clearance and biodistribution against unlabeled and ^{125}I antibodies and found the dye altered the pharmacokinetics. In this study, they used 800CW with a DOL of 1.2−1.4 and showed high liver uptake and faster plasma clearance than radiolabeled or ELISA measurements. Our results are consistent with these findings, where labeling with 800CW can increase plasma clearance at times longer than 4 days. Mouse liver has been shown to take up proteins with a high negative charge density;[5,48] therefore, it is paramount to keep a low DoL (for both fluorophores and radiolabels) to minimize possible alteration of protein pharmacokinetics. Additionally, disruption of FcRn or FcRγ binding could result in faster clearance or altered antibody distribution. Although the exact mechanism of the altered distribution is unclear, our work suggests a 0.3 DoL results in an undetectable difference in antibody pharmacokinetics. Importantly, we examined the pharmacokinetics and biodistribution in healthy animals, while these antibodies will likely be used in animals with tumors, where TMDD may play a role. However, the similar clearance (Figures 2, 3), biodistribution (Figure 5), and microscopic tumor distribution (Figures 6, S5)[18] suggest the labeled antibodies accurately capture the pharmacokinetics of unlabeled antibody.

The published studies on the biodistribution of various antibodies and other proteins with 800CW and encouraging plasma clearance results with AF680 warranted a comparison of the dye effects on the measured biodistribution. For both Bev-800CW and Bev-AF680 at a 0.3 DoL, the plasma clearance was not significantly different at 48 h from unlabeled antibodies (measured with ELISA), prompting us to compare the systemic biodistribution. The biodistribution measured with both dyes (Figure 5a) agreed well for organs where there was sufficient signal intensity relative to autofluorescence variability (liver and kidney); however, the SNR was too low in several other organs to distinguish the signal from the higher background for AF680. The Bev-800CW 48 h biodistribution agreed well with another published biodistribution study using the residualizing ^{64}Cu labeled bevacizumab at 48 h, supporting the aforementioned studies showing similar antibody disposition at low DoL.[30] These data also qualitatively agree with other published biodistribution data of bevacizumab,[25,49] although in some of these studies the mice were exsanguinated (resulting in less measured organ uptake) or the biodistribution measurements were performed at different times post injection, making direct comparisons difficult. For imaging agents, 800CW provides a superior SNR and contrast to noise ratio (CNR) compared to AF680, making it a more suitable choice for live *in vivo* imaging.

Despite the higher autofluorescence in the 680 nm range, the signal from AF680 is sufficient to detect in targeted tumors for several days at clinical doses (Figure 6). Both AF680 and 800CW can be detected in tumors using fresh-frozen tissue sectioning. Here we used thicker (16 μm) slices versus a more typical 5 μm slice thickness to improve signal detection. Both dyes can be excited with a 635 and 750 nm laser, respectively (∼40% of the maximum absorption for AF680 and 55−60% of

DOI: 10.1021/acs.molpharmaceut.6b01091
Mol. Pharmaceutics 2017, 14, 1623−1633

the maximum absorption for 800CW) and detected with photomultiplier tubes. Since both dyes are residualizing, the signal results from the total targeted antibody, in contrast to Fc labeling (Figure S5), for example,[50] which only labels intact protein. This can be useful for applications such as studying ADC's, where the degraded antibody correlates with the released payload (e.g., noncleavable, impermeable small molecules), so NIR detection can be used as a surrogate for small-molecule delivery.[51]

We examined two dyes in detail for this study based on their current use in clinical trials (800CW) and the low plasma protein binding (and associated low nonspecific dye interactions) of AF680.[28] There are a variety of other NIR dyes with different physicochemical properties that are commercially available, although not all of them have disclosed structures. For example, our lab has examined the residualization rates, permeability, and plasma protein binding of several NIR dyes.[27,28] Although some of these fluorophores may have similar properties *in vitro*, their *in vivo* behavior may differ significantly. We have shown that the zwitterionic dye ZW800 has similar plasma protein binding as AF680[28] and beneficial rapid clearance when conjugated to small molecule imaging agents, consistent with literature reports.[52] Additionally, its fluorescence is in the optimal 800 nm range. However, in contrast to labeling small molecules, after conjugation to an antibody, there was a gradual change in the absorbance spectra upon incubation in plasma and a rapid loss of fluorescent signal after injecting *in vivo* (data not shown). In our hands, therefore, this dye is more suitable for rapidly cleared imaging agents than monoclonal antibodies. This result emphasizes that although the structures of other cyanine based dyes (Cy5.5, SulfoCy7, etc.) may be similar to AF680 and 800CW, they each affect antibody disposition differently (e.g., refs 16 and 26). Similar to radiolabeling techniques, the modification of any protein, however slight, can affect different proteins in unique ways, particularly if the modified residue (e.g., lysine, cysteine, tyrosine, etc.) is located in an important binding region for that molecule. The slow clearance of antibodies and complex interactions with the immune system and the FcRn receptor make them sensitive even to small interactions from fluorophores or surface residues/charges.[53−55] The conjugation of fluorophores to smaller proteins or agents may not have much of an impact on the distribution if they are rapidly cleared by the kidneys,[6] but similar methods of validation for distribution should be employed. This work can be used to help guide the selection of fluorophores depending on the particular application in a manner analogous to the selection of chelators and radioisotopes for radiolabeling techniques.

In conclusion, to limit the impact of non-site-specific fluorophore labeling on antibody pharmacokinetics, these results show that the DoL should be kept at or below 0.3 dyes/antibody. At this tracer DoL, AF680 showed negligible impact on plasma clearance out to 17 days compared to unlabeled antibody, while 800CW showed similar clearance out to 4 days but faster clearance at later times. Both dyes can be used with tissue distribution studies; however, the greater autofluorescence for AF680 requires higher doses to achieve a sufficient SNR while the signal from 800CW is well above the autofluorescence background in the 800 nm range. For short-term *in vivo* studies (less than 4 days), the reduced autofluorescence, greater SNR and CNR, and increased tissue penetration of light for 800CW make it suitable for tissue biodistribution studies or live *in vivo* imaging. Although both dyes have distinct advantages and limitations, the efficient optical properties, stability, ease of use, and low autofluorescence for both fluorophores provide broad utility in studying protein pharmacokinetics in the preclinical setting.

■ ASSOCIATED CONTENT

Supporting Information

The Supporting Information is available free of charge on the ACS Publications website at DOI: 10.1021/acs.molpharmaceut.6b01091.

Antibody-dye characterization, including absorbance spectra, serum stability, biexponential fits using PRISM, SDS-PAGE of serum stability and plasma samples, plasma clearance absolute concentration time course, organ scans, and direct antibody labeling versus immunofluorescence detection of intact antibody (PDF)

■ AUTHOR INFORMATION

Corresponding Author

*E-mail: gthurber@umich.edu. Address: 2800 Plymouth Rd., Ann Arbor, MI 48105. Telephone: 734-764-8722.

ORCID

Greg M. Thurber: 0000-0001-7570-2080

Notes

The authors declare no competing financial interest.

■ ACKNOWLEDGMENTS

We would like to thank Eli Lilly for providing funding for the studies. Research reported in this publication was supported by the National Cancer Institute of the National Institutes of Health under Award Number P30CA046592 by the use of the following Cancer Center Shared Resource(s): histology. The content is solely the responsibility of the authors and does not necessarily represent the official views of the National Institutes of Health.

■ REFERENCES

(1) Reichert, J. M. Antibodies to watch in 2016. *mAbs* **2016**, *8*, 197−204.

(2) Boswell, C. A.; Bumbaca, D.; Fielder, P. J.; Khawli, L. A. Compartmental tissue distribution of antibody therapeutics: experimental approaches and interpretations. *AAPS J.* **2012**, *14* (3), 612−618.

(3) Zhang, L.; Navaratna, T.; Thurber, G. M. A Helix-Stabilizing Linker Improves Subcutaneous Bioavailability of a Helical Peptide Independent of Linker Lipophilicity. *Bioconjugate Chem.* **2016**, *27*, 1663−1672.

(4) Goldenberg, D. M.; Larson, S. M. Radioimmunodetection in cancer identification. *J. Nucl. Med.* **1992**, *33* (5), 803−814.

(5) Boswell, C. A.; Tesar, D. B.; Mukhyala, K.; Theil, F.-P.; Fielder, P. J.; Khawli, L. A. Effects of Charge on Antibody Tissue Distribution and Pharmacokinetics. *Bioconjugate Chem.* **2010**, *21* (12), 2153−2163.

(6) Conner, K. P.; Rock, B. M.; Kwon, G. K.; Balthasar, J. P.; Abuqayyas, L.; Wienkers, L. C.; Rock, D. A. Evaluation of near infrared fluorescent labeling of monoclonal antibodies as a tool for tissue distribution. *Drug Metab. Dispos.* **2014**, *42*, 1906−1913.

(7) Boswell, C. A.; Mundo, E. E.; Zhang, C.; Bumbaca, D.; Valle, N. R.; Kozak, K. R.; Fourie, A.; Chuh, J.; Koppada, N.; Saad, O.; Gill, H.; Shen, B. Q.; Rubinfeld, B.; Tibbitts, J.; Kaur, S.; Theil, F. P.; Fielder, P. J.; Khawli, L. A.; Lin, K. Impact of drug conjugation on pharmacokinetics and tissue distribution of Anti-STEAP1 antibody-drug conjugates in rats. *Bioconjugate Chem.* **2011**, *22*, 1994−2004.

DOI: 10.1021/acs.molpharmaceut.6b01091
Mol. Pharmaceutics 2017, 14, 1623−1633

(8) Hoppin, J.; Orcutt, K. D.; Hesterman, J. Y.; Silva, M. D.; Cheng, D.; Lackas, C.; Rusckowski, M. Assessing antibody pharmacokinetics in mice with in vivo imaging. *J. Pharmacol. Exp. Ther.* **2011**, *337* (2), 350−358.
(9) Natarajan, A.; Türkcan, S.; Gambhir, S. S.; Pratx, G. Multiscale Framework for Imaging Radiolabeled Therapeutics. *Mol. Pharmaceutics* **2015**, *12*, 4554.
(10) Weissleder, R.; Ntziachristos, V. Shedding light onto live molecular targets. *Nat. Med.* **2003**, *9*, 123−128.
(11) Vahrmeijer, A. L.; Hutteman, M.; Van Der Vorst, J. R.; Van De Velde, C. J. H.; Frangioni, J. V. Image-guided cancer surgery using near-infrared fluorescence. *Nat. Rev. Clin. Oncol.* **2013**, *10*, 507−518.
(12) Gioux, S.; Choi, H. S.; Frangioni, J. V. Image-guided surgery using invisible near-infrared light: Fundamentals of clinical translation. *Mol. Imaging* **2010**, *9*, 237−255.
(13) de Vries, E. G. E.; Munnink, T. H. O.; van Vugt, M. a. T. M.; Nagengast, W. B. Toward molecular imaging-driven drug development in oncology. *Cancer Discovery* **2011**, *1*, 25−28.
(14) Maeda, A.; Bu, J.; Chen, J.; Zheng, G.; DaCosta, R. S. Dual in vivo Photoacoustic and Fluorescence Imaging of HER2 Expression in Breast Tumors for Diagnosis, Margin Assessment, and Surgical Guidance. *Mol. Imaging* **2015**, *14* (1), 1−9.
(15) Zhang, L.; Navaratna, T.; Liao, J.; Thurber, G. M. Dual-purpose linker for alpha helix stabilization and imaging agent conjugation to glucagon-like peptide-1 receptor ligands. *Bioconjugate Chem.* **2015**, *26*, 329−337.
(16) Sato, K.; Nagaya, T.; Nakamura, Y.; Harada, T.; Nani, R. R.; Shaum, J. B.; Gorka, A. P.; Kim, I.; Paik, C. H.; Choyke, P. L.; Schnermann, M. J.; Kobayashi, H. Impact of C4′- O -Alkyl Linker on in Vivo Pharmacokinetics of Near-Infrared Cyanine/Monoclonal Antibody Conjugates. *Mol. Pharmaceutics* **2015**, *12*, 3303−3311.
(17) Darne, C.; Lu, Y.; Sevick-Muraca, E. M. Small animal fluorescence and bioluminescence tomography: a review of approaches, algorithms and technology update. *Phys. Med. Biol.* **2014**, *59* (1), R1−R64.
(18) Cilliers, C.; Guo, H.; Liao, J.; Christodolu, N.; Thurber, G. M. Multiscale Modeling of Antibody-Drug Conjugates: Connecting Tissue and Cellular Distribution to Whole Animal Pharmacokinetics and Potential Implications for Efficacy. *AAPS J.* **2016**, *18* (5), 1117−1130.
(19) Oliveira, S.; Cohen, R.; Walsum, M. S.-v.; van Dongen, G. A.; Elias, S. G.; van Diest, P. J.; Mali, W.; van Bergen En Henegouwen, P. M. A novel method to quantify IRDye800CW fluorescent antibody probes ex vivo in tissue distribution studies. *EJNMMI Res.* **2012**, *2*, 50.
(20) Cohen, R.; Vugts, D. J.; Stigter-van Walsum, M.; Visser, G. W. M.; van Dongen, G. a. M. S. Inert coupling of IRDye800CW and zirconium-89 to monoclonal antibodies for single- or dual-mode fluorescence and PET imaging. *Nat. Protoc.* **2013**, *8* (5), 1010−1018.
(21) Bhatnagar, S.; Deschenes, E.; Liao, J.; Cilliers, C.; Thurber, G. M. Multichannel Imaging to Quantify Four Classes of Pharmacokinetic Distribution in Tumors. *J. Pharm. Sci.* **2014**, *103*, 3276−3286.
(22) Rogers, B. E.; Franano, F. N.; Edwards, W. B.; Connett, J. M.; Anderson, C. J.; Duncan, J. R.; Welch, M. J. Identification of Metabolites of 111In-Diethylenetriaminepentaacetic Acid Monoclonal Antibodies and Antibody Fragments in Vivo. *Cancer Res.* **1995**, *55*, 5714s−5720s.
(23) Sands, H. Experimental studies of radioimmunodetection of cancer: an overview. *Cancer Res.* **1990**, *50*, 809s−813s.
(24) Brechbiel, M. W.; Gansow, O. A.; Atcher, R. W.; Schlom, J.; Esteban, J.; Simpson, D.; Colcher, D. Synthesis of 1-(p-isothiocyanatobenzyl) derivatives of DTPA and EDTA. Antibody labeling and tumor-imaging studies. *Inorg. Chem.* **1986**, *25*, 2772−2781.
(25) Cohen, R.; Stammes, M. A.; de Roos, I. H.; Stigter-van Walsum, M.; Visser, G. W.; van Dongen, G. A. Inert coupling of IRDye800CW to monoclonal antibodies for clinical optical imaging of tumor targets. *EJNMMI Res.* **2011**, *1* (1), 31.
(26) Sato, K.; Gorka, A. P.; Nagaya, T.; Michie, M. S.; Nani, R. R.; Nakamura, Y.; Coble, V. L.; Vasalatiy, O. V.; Swenson, R. E.; Choyke, P. L.; Schnermann, M. J.; Kobayashi, H. Role of Fluorophore Charge on the in Vivo Optical Imaging Properties of Near-Infrared Cyanine Dye/Monoclonal Antibody Conjugates. *Bioconjugate Chem.* **2016**, *27*, 404−413.
(27) Cilliers, C.; Liao, J.; Atangcho, L.; Thurber, G. M. Residualization Rates of Near-Infrared Dyes for the Rational Design of Molecular Imaging Agents. *Mol. Imaging Biol.* **2015**, *17* (6), 757−762.
(28) Zhang, L.; Bhatnagar, S.; Deschenes, E.; Thurber, G. M. Mechanistic and quantitative insight into cell surface targeted molecular imaging agent design. *Sci. Rep.* **2016**, *6*, 25424.
(29) Zhang, L.; Thurber, G. M. Quantitative Impact of Plasma Clearance and Down-regulation on GLP-1 Receptor Molecular Imaging. *Mol. Imaging Biol.* **2016**, *18*, 79−89.
(30) Paudyal, B.; Paudyal, P.; Oriuchi, N.; Hanaoka, H.; Tominaga, H.; Endo, K. Positron emission tomography imaging and biodistribution of vascular endothelial growth factor with 64Cu-labeled bevacizumab in colorectal cancer xenografts. *Cancer Sci.* **2011**, *102*, 117−121.
(31) Trotter, M. J.; Chaplin, D. J.; Olive, P. L. Use of a Carbocyanine Dye as a Marker of Functional Vasculature in Murine Tumors. *Br. J. Cancer* **1989**, *59* (5), 706−709.
(32) Harris, L. J.; Skaletsky, E.; McPherson, A. Crystallographic structure of an intact IgG1 monoclonal antibody1. *J. Mol. Biol.* **1998**, *275*, 861−872.
(33) Wishart, D. S.; Knox, C.; Guo, A. C.; Shrivastava, S.; Hassanali, M.; Stothard, P.; Chang, Z.; Woolsey, J. DrugBank: a comprehensive resource for in silico drug discovery and exploration. *Nucleic Acids Res.* **2006**, *34*, D668−D672.
(34) Ogawa, M.; Regino, C. A. S.; Choyke, P. L.; Kobayashi, H. In vivo target-specific activatable near-infrared optical labeling of humanized monoclonal antibodies. *Mol. Cancer Ther.* **2009**, *8*, 232−239.
(35) Aldrich, M. B.; Wang, X.; Hart, A.; Kwon, S.; Sampath, L.; Marshall, M. V.; Sevick-Muraca, E. M. Assessment of free dye in solutions of dual-labeled antibody conjugates for in vivo molecular imaging. *Mol. Imaging Biol.* **2011**, *13*, 32−42.
(36) Sako, Y.; Minoghchi, S.; Yanagida, T. Single-molecule imaging of EGFR signalling on the surface of living cells. *Nat. Cell Biol.* **2000**, *2*, 168−172.
(37) Kim, M. T.; Chen, Y.; Marhoul, J.; Jacobson, F. Statistical modeling of the drug load distribution on trastuzumab emtansine (Kadcyla), a lysine-linked antibody drug conjugate. *Bioconjugate Chem.* **2014**, *25*, 1223−1232.
(38) Goldmacher, V. S.; Amphlett, G.; Wang, L.; Lazar, A. C. Statistics of the distribution of the abundance of molecules with various drug loads in maytansinoid antibody-drug conjugates. *Mol. Pharmaceutics* **2015**, *12*, 1738−1744.
(39) Austin, C. D.; De Maziere, A. M.; Pisacane, P. I.; van Dijk, S. M.; Eigenbrot, C.; Sliwkowski, M. X.; Klumperman, J.; Scheller, R. H. Endocytosis and sorting of ErbB2 and the site of action of cancer therapeutics trastuzumab and geldanamycin. *Mol. Biol. Cell* **2004**, *15* (12), 5268−5282.
(40) Thurber, G. M.; Schmidt, M. M.; Wittrup, K. D. Antibody tumor penetration: Transport opposed by systemic and antigen-mediated clearance. *Adv. Drug Delivery Rev.* **2008**, *60* (12), 1421−1434.
(41) Ito, S.; Muguruma, N.; Hayashi, S.; Taoka, S.; Bando, T.; Inayama, K.; Sogabe, M.; Okahisa, T.; Okamura, S.; Shibata, H.; Irimura, T.; Takesako, K.; Shibamura, S. Development of agents for reinforcement of fluorescence on near-infrared ray excitation for immunohistological staining. *Bioorg. Med. Chem.* **1998**, *6*, 613−618.
(42) Gioux, S.; Choi, H. S.; Frangioni, J. V. Image-guided surgery using invisible near-infrared light: fundamentals of clinical translation. *Mol. Imaging* **2010**, *9* (5), 237−55.
(43) Thurber, G. M.; Figueiredo, J.-L.; Weissleder, R. Detection limits of intraoperative near infrared imaging for tumor resection. *J. Surg. Oncol.* **2010**, *102*, 758−764.
(44) Hamblett, K. J.; Senter, P. D.; Chace, D. F.; Sun, M. M. C.; Lenox, J.; Cerveny, C. G.; Kissler, K. M.; Bernhardt, S. X.; Kopcha, A.

DOI: 10.1021/acs.molpharmaceut.6b01091
Mol. Pharmaceutics 2017, 14, 1623−1633

K.; Zabinski, R. F.; Meyer, D. L.; Francisco, J. A. Effects of Drug Loading on the Antitumor Activity of a Monoclonal Antibody Drug Conjugate. *Clin. Cancer Res.* **2004**, *10* (20), 7063−7070.
(45) Lyon, R. P.; Bovee, T. D.; Doronina, S. O.; Burke, P. J.; Hunter, J. H.; Neff-LaFord, H. D.; Jonas, M.; Anderson, M. E.; Setter, J. R.; Senter, P. D. Reducing hydrophobicity of homogeneous antibody-drug conjugates improves pharmacokinetics and therapeutic index. *Nat. Biotechnol.* **2015**, *33*, 733−736.
(46) Junutula, J. R.; Raab, H.; Clark, S.; Bhakta, S.; Leipold, D. D. D.; Weir, S.; Chen, Y.; Simpson, M.; Tsai, S. P. S. P.; Dennis, M. S. M. S.; Lu, Y.; Meng, Y. G.; Ng, C.; Yang, J.; Lee, C. C.; Duenas, E.; Gorrell, J.; Katta, V.; Kim, A.; McDorman, K.; Flagella, K.; Venook, R.; Ross, S.; Spencer, S. D.; Lee Wong, W.; Lowman, H. B.; Vandlen, R.; Sliwkowski, M. X.; Scheller, R. H.; Polakis, P.; Mallet, W.; et al. Site-specific conjugation of a cytotoxic drug to an antibody improves the therapeutic index. *Nat. Biotechnol.* **2008**, *26*, 925−932.
(47) Lyon, R. P.; Setter, J. R.; Bovee, T. D.; Doronina, S. O.; Hunter, J. H.; Anderson, M. E.; Balasubramanian, C. L.; Duniho, S. M.; Leiske, C. I.; Li, F.; Senter, P. D. Self-hydrolyzing maleimides improve the stability and pharmacological properties of antibody-drug conjugates. *Nat. Biotechnol.* **2014**, *32*, 1059−1062.
(48) Yamasaki, Y.; Sumimoto, K.; Nishikawa, M.; Yamashita, F.; Yamaoka, K.; Hashida, M.; Takakura, Y. Pharmacokinetic analysis of in vivo disposition of succinylated proteins targeted to liver non-parenchymal cells via scavenger receptors: importance of molecular size and negative charge density for in vivo recognition by receptors. *J. Pharmacol. Exp. Ther.* **2002**, *301*, 467−477.
(49) Van Der Bilt, A. R. M.; Terwisscha Van Scheltinga, A. G. T.; Timmer-Bosscha, H.; Schröder, C. P.; Pot, L.; Kosterink, J. G. W.; Van Der Zee, A. G. J.; Lub-de Hooge, M. N.; De Jong, S.; De Vries, E. G. E.; Reyners, A. K. L. Measurement of tumor VEGF-A levels with 89Zr-bevacizumab PET as an early biomarker for the antiangiogenic effect of everolimus treatment in an ovarian cancer xenograft model. *Clin. Cancer Res.* **2012**, *18*, 6306−6314.
(50) Baker, J.; Lindquist, K.; Huxham, L.; Kyle, A.; Sy, J.; Minchinton, A. Direct Visualization of Heterogeneous Extravascular Distribution of Trastuzumab in Human Epidermal Growth Factor Receptor Type 2 Overexpressing Xenografts. *Clin. Cancer Res.* **2008**, *14* (7), 2171−2179.
(51) Erickson, H. K.; Park, P. U.; Widdison, W. C.; Kovtun, Y. V.; Garrett, L. M.; Hoffman, K.; Lutz, R. J.; Goldmacher, V. S.; Blattler, W. A. Antibody-maytansinoid conjugates are activated in targeted cancer cells by lysosomal degradation and linker-dependent intracellular processing. *Cancer Res.* **2006**, *66* (8), 4426−4433.
(52) Choi, H. S.; Gibbs, S. L.; Lee, J. H.; Kim, S. H.; Ashitate, Y.; Liu, F. B.; Hyun, H.; Park, G.; Xie, Y.; Bae, S.; Henary, M.; Frangioni, J. V. Targeted zwitterionic near-infrared fluorophores for improved optical imaging. *Nat. Biotechnol.* **2013**, *31* (2), 148−153.
(53) Kelly, R. L.; Sun, T.; Jain, T.; Caffry, I.; Yu, Y.; Cao, Y.; Lynaugh, H.; Brown, M.; Vasquez, M.; Wittrup, K. D.; Xu, Y. High throughput cross-interaction measures for human IgG1 antibodies correlate with clearance rates in mice. *MAbs* **2015**, *7* (4), 770−777.
(54) Geng, S. B.; Cheung, J. K.; Narasimhan, C.; Shameem, M.; Tessier, P. M. Improving monoclonal antibody selection and engineering using measurements of colloidal protein interactions. *J. Pharm. Sci.* **2014**, *103* (11), 3356−3363.
(55) Hotzel, I.; Theil, F. P.; Bernstein, L. J.; Prabhu, S.; Deng, R.; Quintana, L.; Lutman, J.; Sibia, R.; Chan, P.; Bumbaca, D.; Fielder, P.; Carter, P. J.; Kelley, R. F. A strategy for risk mitigation of antibodies with fast clearance. *MAbs* **2012**, *4* (6), 753−760.

DOI: 10.1021/acs.molpharmaceut.6b01091
Mol. Pharmaceutics 2017, 14, 1623−1633